Chemical Physics Letters 500 (2010) 54–58

Contents lists available at ScienceDirect

Chemical Physics Letters

journal homepage: www.elsevier.com/locate/cplett

Assignment of the He@C_{84} isomers in experimental NMR spectra using density functional calculations

Petr Štěpánek [a,b], Petr Bouř [a], Michal Straka [a,*]

[a] Institute of Organic Chemistry and Biochemistry, Academy of Sciences, Flemingovo nám 2, 166 10 Prague, Czech Republic
[b] Institute of Physics, Charles University, Ke Karlovu 5, Prague 2, 121 16, Czech Republic

ARTICLE INFO

Article history:
Received 23 June 2010
In final form 23 September 2010
Available online 27 September 2010

ABSTRACT

The ^{3}He chemical shifts were calculated for He$_n$@C_{84} (n = 1, 2) fullerenes to obtain characteristic NMR patterns for distinguishing their isomers in a mixture. The density functional methods were calibrated on experimental data. Accuracy within 1 ppm could be reached without further fitting of individual shifts. Such precision allows for a semi-quantitative assignment of ^{3}He NMR spectra. Additional criteria in the identification are discussed, such as the relative energies of the isomers, positions of the satellite di-helium peaks, and the differential ^{3}He shifts in the fullerenes reduced to anions. Endohedral ^{3}He shifts are predicted for so far experimentally unknown He@C_{84} and He@C_{84}^{6-} isomers.

1. Introduction

Fullerenes are molecules of spherical or ellipsoidal shape formed by tens to hundreds of carbon atoms. Typically, they form a large number of isomers. For the cage of the title species, C_{84}, 24 possible isolated pentagon rule (IPR) [1] isomers were predicted. Of them, at least 10 have been observed experimentally [2–4]. Fullerenes are usually prepared by extraction of arc-processed soot, typically in relatively small amounts as a mixture of different fullerenes and their isomers. Separation and a consequent identification is thus an important part of fullerene chemistry, typically based on chromatographic methods (HPLC) coupled with mass spectroscopy, ^{13}C NMR, etc.

Helium atom(s) can be introduced into the fullerene cage under elevated temperatures and pressures [5]. Mono- and di-helium species can be produced in this way. The inert helium atom presents an excellent NMR probe as the ^{3}He NMR shift is extremely sensitive to the size, shape, and substitution of the cage in which the atom is enclosed [6–8]. One can also follow chemical reactions of fullerenes using the helium labelling [9]. Owing to the excellent resolution of ^{3}He NMR (10^{-3} ppm) spectroscopy the ^{3}He isotropic shift can help in distinguishing between different fullerene cages, isomers, or differently substituted fullerenes. However, the ^{3}He itself does not tell us anything about the fullerene cage and its shape or substitution. The electronic structure calculations thus provide a welcome additional method to determine the cage geometry, together with more classical approaches, such as mass or powder X-ray spectroscopy.

In numerous computational studies of ^{3}He NMR shifts in endohedral helium fullerenes, due to the high computational cost involved, relatively modest computational levels (semi-empirical, HF) and density functional theory (DFT) methods have been used. Moreover, the computations have been restricted to small basis sets (3-21G, DZP, 6-31G*) [10–17]. Despite the approximate levels employed, the calculations were able to provide a good qualitative insight into the NMR–structure relationship. An important step towards a better agreement between the theory and experiment is the approach of Wang et al. based on the scaling the computational results (semi-empirical AM1 or PM3 geometries and HF/3-21G or B3LYP/3-21G chemical shifts) on experimentally known data, and using the scaled values for predictive and explanatory purposes [16,17]. Herein, we should also mention the pioneering work of Hadon and Pasquarello [18].

In this study, following Ref. [19], we employ density functional methods to interpret experimental ^{3}He NMR spectra of He$_n$@C_{84} (n = 1, 2) isomers in a mixture of endohedral helium fullerenes [20,21]. Of the He@C_{84} isomers, only signals for isomer No:4(D_{2d}) at −24.354 ppm and No:22(D_2) at −8.957 ppm could be assigned experimentally [13,21]. We have recently shown that DFT approaches can provide reliable computational data for ^{3}He endohedral shifts in endohedral helium fullerenes [19]. Employing a model He@C_{60} system we found out that the BHandHLYP functional with def-TZVP basis sets provided computational shifts within 1 ppm of the experimental ones. The good performance of the BHandHLYP functional for noble gas NMR shifts was confirmed also in studies of $^{129/131}$Xe NMR shift in weakly-bonded Xe systems [22,23].

Wang and Wu have lately reported computational assignment of the ^{3}He NMR spectra of mixture of endohedral fullerenes [17] reported experimentally in Ref. [20] using the scaling approach of

* Corresponding author.
E-mail address: straka@uochb.cas.cz (M. Straka).

0009-2614/$ - see front matter © 2010 Elsevier B.V. All rights reserved.
doi:10.1016/j.cplett.2010.09.061

Ref. [16]. In the present work the scaling of computational results according to the experimental data could be avoided and results of the same quality were obtained (Section 3.2). We further attempt to reproduce the small differences between the mono- and di-helium peaks using the position of a satellite peak as a further parameter in identification of corresponding isomers (Section 3.2). We discuss the possibility of using the ^{3}He NMR shifts in reduced endohedral helium fullerenes to improve the assignment. Hexa-anionic He@C_{84}^{6-} are calculated and compared to the neutral ones (Section 3.3). Predictions of ^{3}He NMR shift are provided for the so far unsynthesized He@C_{84} isomers and their reduced hexa-anionic counterparts.

2. Computational details

2.1. Methods

The TURBOMOLE 5.10 program [24] was employed in the calculations. The DFT BP86 functional [25,26] together with the def-TZVP [27] basis set implemented in the TURBOMOLE code were employed in calculations of minimum-energy structures. The resolution-of-identity (RI) approximation [28] was used in the structure optimisations. The BHandHLYP [25,29,30] functional together with the def-TZVP basis set was employed in the calculations of ^{3}He shielding. The Gauge-Including Atomic Orbitals (GIAO) was used to treat the gauge dependence in the shielding calculations. The shieldings were turned into shifts using isolated helium atom as a reference: $\delta(^3\mathrm{He}_n@\mathrm{C}_{84}) = \sigma(^3\mathrm{He}) - \sigma(^3\mathrm{He}@\mathrm{C}_{84})$. The threshold and convergence parameters of the TURBOMOLE code were tightened in the shielding calculations (*gridsize* m5 and *scfconv* 10^{-8}) to reduce numerical noise.

2.2. Minimum structures

Helium atom was placed at the center of mass of each cage and the structures were optimised at the BP86/def-TZVP level maintaining the symmetry of corresponding C_{84} isomers. The optimised structures were verified by calculating of harmonic vibrational frequencies (not shown). Several isomers showed one or more negative frequencies of a few cm^{-1} corresponding to helium motions in the fullerene cage. This can be ascribed to the shallow potential inside the cage in a combination with numerical DFT errors. An additional check with shifting the coordinates along the negative modes and re-running the structure optimisations typically led to only very marginal changes in the electronic energy (ca. 0.01 kJ/mol) and calculated ^{3}He shifts (ca. 0.01 ppm). Isomer He@C_{84}:10 did not converge to a minimum. Corresponding C_{84}:10 cage has been reported to be problematic, see e.g., Ref. [31]. We excluded He@C_{84}:10 from our study.

In the di-helium systems, where the weak potential for two helium atoms inside a C_{84} cage caused a very poor convergence in the structure optimisations, we used following strategy: The two helium atoms were put symmetrically around the center of the mass of the cage along either *x*, or *y*, or *z* axis with $r_{\mathrm{He-He}} \sim 2$ Å and the resulting structure was optimised. The lowest minima were then used in the ^{3}He NMR shift calculations.

3. Results and discussion

3.1. Calibration

Similarly as in Ref. [19] we calibrate the performance of the approach on the experimentally identified helium fullerenes. Figure 1 shows the calculated (BHandHLYP/def-TZVP) and experimental ^{3}He NMR shifts for a set of endohedral helium systems, from

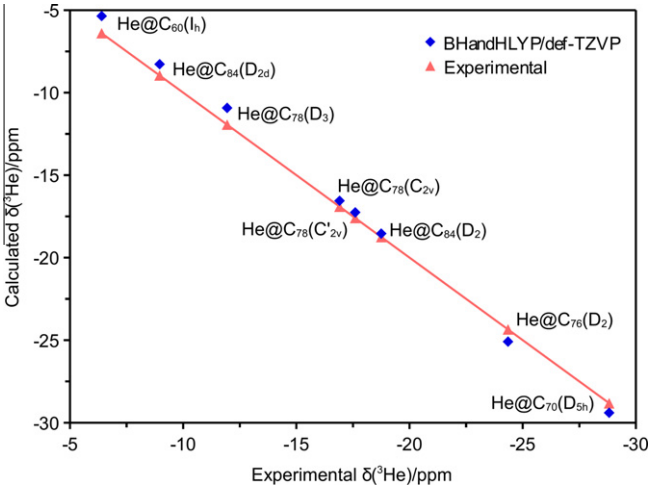

Figure 1. Calculated vs. experimental ^{3}He NMR shifts in a series of endohedral helium fullerenes.

He@C_{60} through He@C_{78}, using the BP86/def-TZVP geometries. The two previously assigned He@C_{84} isomers, No:22 and No:4 are also added in Figure 1. The performance of the BHandHLYP/def-TZVP method is apparently uniform and stable for all the included fullerenes of different shape and size. The correlation coefficient for the theoretical and experimental values included in the plot is 0.9992. Interestingly, the theory tends to systematically underestimate the experiment at lower values of ^{3}He shift, and to overestimate them at larger values. This may be utilized in further assignment. The largest deviation from the experiment, 1.01 ppm, is obtained for the isomer He@C_{78}:1(D_3). The errors expected in the calculations on different He@C_{84} thus can be expected to lie in the interval ±1 ppm. However, this apparently good computational accuracy is not enough to fully reproduce the relatively tight spacing of the endohedral ^{3}He shifts (Table 1, some of the fullerenes and isomers differ by less than 1 ppm in the ^{3}He shift). Hence, additional criteria have to be used in the assignment as discussed below. However, unlike previous approaches, the BHandHLYP/def-TZVP results do not need to be empirically scaled.

3.2. The He@C_{84} family

3.2.1. Structures

It has been shown that, already for the smaller He@C_{60} complex, the energy and chemical shielding hypersurfaces near the center of the cage are nearly flat [32,33]. Moreover, the energy hypersurface raises substantially faster towards the walls than the shielding hypersurface [32]. While one can expect that the He atom will move almost freely in a certain region near the center of the cage, possible dynamical effects on the ^{3}He shift are expected to be small because places with increased shielding are not energetically favourable. We have shown recently that for an analogous system Xe@C_{60} the effects of dynamics on ^{129}Xe NMR shift in a rigid C_{60} cage were small, about 0.5 ppm of the total shift of 130 ppm [22]. Hence, we neglected the dynamical effects in the present calculations and used structures with He at the center of mass of the cage. We also note that the presence of one or two He atoms in a cage has negligible effect on the geometry of the cage [19].

3.2.2. ^{3}He chemical shifts

The calculated ^{3}He chemical shifts for the 23 isomers of He@C_{84} are listed in Table 1, together with the experimental values from Ref. [20] assigned in this Letter. Because of the computational

Table 1
Calculated[a] ^{3}He NMR shifts (ppm) and relative energies (kJ/mol) of 23 isomers of He@C_{84}. Corresponding values for selected He_2@C_{84} isomers in parentheses. Results from Ref. [17] are given for comparison.[b] Calculated[a] ^{3}He NMR shifts (ppm) for He@C_{84}^{6-} anions.

Isomer	Point group	He_n@C_{84}			Wang and Wu[b]	He@C_{84}^{6-}
		δ_{calc}	δ_{exp}	ΔE[c]	δ_{corr}	δ_{calc}
1	D_2	−17.66		207.8	−18.01	−30.44
2	C_2	−18.58		128.5	−18.90	−11.18
3	C_s	−3.49		115.2	0.49	−23.67
4	D_{2d}	−25.01 (−24.81)	−24.354	51.4	−24.68	−18.99
5	D_2	−18.52		56.4	−18.45	−20.24
6	C_{2v}	−5.86		67.8	−5.00	−25.30
7	C_{2v}	−3.02		89.6	−2.14	−26.34
8	C_2	−7.14		72.1	−6.56	−25.30
9	C_2	−3.09		97.5	4.43	−24.22
11	C_2	−6.83 (−7.28)	−7.502 (−7.539)	33.5	−6.10	−19.64
12	C_1	−5.03		44.1	−4.32	−25.30
13	C_2	3.85		92.0	5.89	−24.75
14	C_s	−10.93 (−11.15)	−11.114	59.5	−11.09	−27.92
15	C_s	−7.75		39.6	−7.35	−25.98
16	C_s	−8.82 (−9.17)	−9.605 (−9.647)	34.0	−8.68	−15.90
17	C_{2v}	−2.43		86.7	−0.40	−23.94
18	C_{2v}	−9.53 (−9.98)	−10.006	67.2	−9.42	−29.05
19	D_{3d}	−3.50		42.8	−1.72	−50.98
20	T_d	−11.96		131.1	−12.38	−52.11
21	D_2	−3.69		55.0	−3.04	−26.28
22	D_2	−8.20 (−8.37)	−8.957	0.0	−8.00	−25.27
23	D_{2d}	−7.81 (−7.53)	−8.404 (−8.369)	1.0	−7.40	−26.20
24	D_{6h}	−12.29		30.0	−12.77	−16.53

[a] At BHandHLYP/def-TZVP//BP86/def-TZVP level.
[b] Scaled B3LYP/3-21G//AM1 results from Ref. [17].
[c] Energy relative to the lowest energy isomer No:22.

accuracy of ±1 ppm and close spacing of the experimental peaks, we used additional criteria in the assignment, namely the relative energy of the isomer and the position of the satellite peaks due to di-helium system, when applicable.

The comparison of electronic energy of the different He@C_{84} isomers is shown in Figure 2. It is important to notice that different computational methods actually provide different energy ordering of the isomers. This may generally become a problem when two isomers are too close in energy. In the present case, it should not alter the resulting assignment. We notice that while the relative energies are useful for assignment of spectra, the formation of fullerene isomers is not an equilibrium process and relative amount of an isomer in a prepared mixture does not depend only on its energy but also on kinetic factors.

The di-helium species can be identified in the ^{3}He-NMR spectrum as minor satellites within hundredths to tenths of ppm in both directions. We have shown previously that at least the sign of the difference between the particular di-helium and mono-helium system, in other words the relative position of the satellite peak in the spectra (shielding, deshielding), can be reproduced [19]. This is due to error cancellation when following differential (di-helium minus mono-helium) ^{3}He shifts. Although the calculated differences for di-helium vs. mono-helium species are 5–10 times larger then the experimental ones (Table 1), the sign of the change is predicted correctly by the calculations, and thus may be utilized in the assignment.

Figures 3 and 4 show schematically how the assignment was done. The vertical lines correspond to the experimental values,

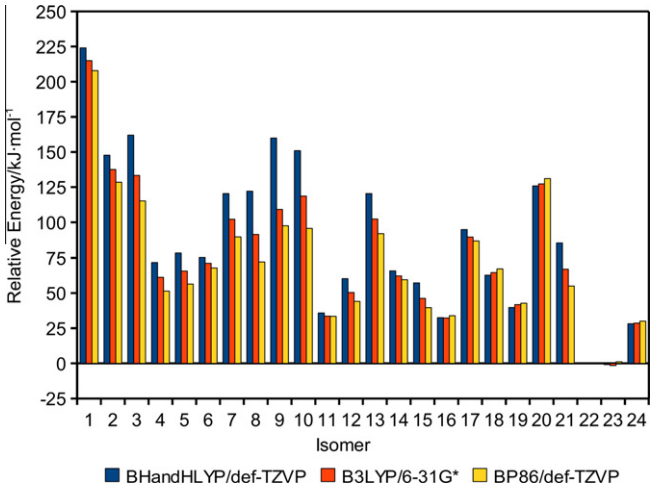

Figure 2. Calculated electronic energies of He@C_{84} isomers relative to the lowest-energy isomer, He@C_{84}:22 at different computational levels. Results of the present work and Ref. [17] (B3LYP/6-31G* data) used.

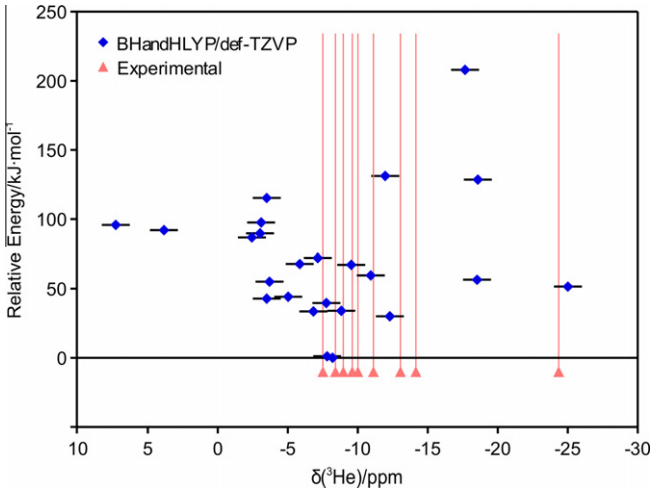

Figure 3. Calculated relative energies vs. ^{3}He NMR shifts (error bars of ±1 ppm) for the He@C_{84} isomers. Vertical lines correspond to the experimental ^{3}He shifts.

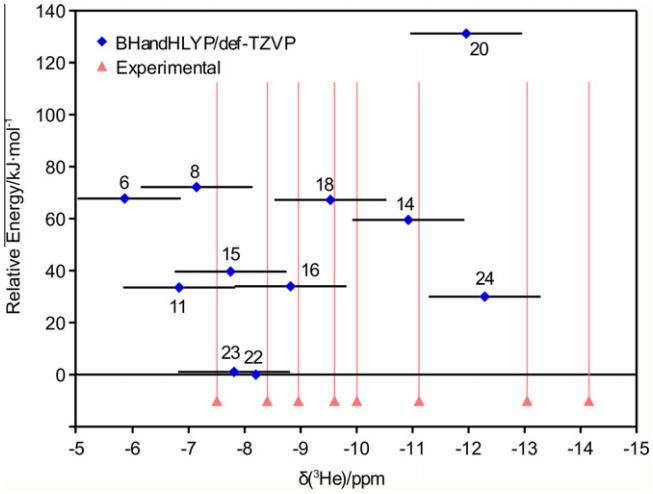

Figure 4. Calculated relative energies vs. ^{3}He NMR shifts (error bars ±1 ppm) for selected He@C_{84} isomers. Vertical lines show the experimental ^{3}He NMR shifts.

the *x*-axis is the ^{3}He shift range and on *y*-axis are the calculated relative energies of isomers. The peak at −7.502 ppm can be assigned to He@C_{84}:11(C_2) with calculated value of −6.83 ppm because of the high energy of the other possible isomer He@C_{84}:8 (Figure 4). The calculated satellite peak at −7.28 ppm (Table 1) for He_2@C_{84}:11 indeed corresponds to more shielding in the di-helium system, in a qualitative agreement with the experiment (−7.539 ppm).

The signal at −8.404 ppm corresponds to He@C_{84}:23(D_{2d}), with calculated value at −7.81 ppm, because the nearby low-energy isomer He@C_{84}:22(D_2) (calculated at −8.20 ppm) was assigned experimentally to the signal at −8.957 ppm, and other candidate, He@C_{84}:15(C_s) is high in energy (Figure 4). Furthermore, no experimental evidence exists for empty C_{84}:15 cage. The intensity of the He@C_{84}:23(D_{2d}) peak is lower than expected from the relative energy of He@C_{84}:23; this can be due to kinetic factors during the formation of the fullerene. The calculated ^{3}He shift for the di-helium He_2@C_{84}:23 of −7.53 ppm is on the deshielding side of the mono-helium one (−7.81 ppm, Table 1), in a qualitative agreement with the experiment (−8.369 vs. −8.404 ppm in Table 1).

The peak at −9.605 ppm can be assigned to He@C_{84}:16(C_s) calculated at −8.82 ppm (Table 1, Figure 4). The calculated value of di-helium isomer (−9.17 ppm) shows more shielding, in a qualitative agreement with the experiment (−9.647 ppm). The signal at −10.006 ppm can be assigned to He@C_{84}:18(C_{2v}), with calculated value −9.53 ppm (Figure 4). We note that isomers He@C_{84}:14 and He@C_{84}:18 are close in the energy (Figure 2 and Figure 4), but the corresponding intensity of the experimental signal was much higher for the He@C_{84}:14 [20]. Different kinetic factors in the formation of these two isomers may play a role. Signal at −11.114 ppm could be assigned either to He@C_{84}:14(C_s) or He@C_{84}:20(T_d), with calculated values of −10.93 and −11.96 ppm (Figure 4), respectively. The He@C_{84}:20 is high in energy (∼130 kJ/mol above the lowest isomer, He@C_{84}:22) and no experimental evidence exists for the corresponding pristine C_{84}:20. Hence the signal at −11.114 ppm is assigned to He@C_{84}:14.

In the experimental spectra [20] the signal at −14.149 ppm was reported as due to He@C_{84} species, while a resonance at −13.046 ppm was tentatively assigned to a He@C_{82}. We observe no calculated resonance near −14.149 ppm, while the signal at −13.046 ppm nicely corresponds to the energetically low-lying He@C_{84}:24 isomer. This is in agreement with the results of Ref. [17] in which the −14.149 ppm was computationally assigned to He@C_{86}:16, and signal at −13.046 ppm to He@C_{84}:24.

We also calculated satellite di-helium signals for the isomers 4, 14, 18, and 22, for which only single mono-helium peaks are observed. The differences between mono- and di-helium calculated values are smaller than those for the isomers with experimentally observed satellites. Exception is isomer 18 for which already the mono-helium signal is small. Hence, we expect the di-helium signal to be lost in the noise. The smaller calculated differences may suggest that the corresponding di-helium signals are too close to the mono-helium ones to be resolved. We, however, cannot exclude the possibility that the di-helium systems are present only in small amounts with the signal hidden in the noise, or that they are not present at all.

In Table 1 we further relate our results to the work of Wang and Wu [17] in which scaled computational B3LYP/3-21G data were used. Both methods give very similar results except for situations when the ^{3}He shifts are small in value, see, e.g., isomers 3, 9, and 17 in Table 1. This may be due to numerical reasons: A small number, chemical shift, is obtained as a difference of large numbers, shielding of the reference He atom (∼59 ppm) minus the shielding of the He@C_{84} isomer in question. No conclusions can be drawn from the present data whether one or another approach is more or less reliable.

3.3. Endohedral helium anions

Experimental studies have shown that if an endohedral helium fullerene is reduced to an anion the shielding in the cage changes substantially and the corresponding anion (typically 6-, but also 4-, see Ref. [19]) resonates at a different frequency [6–8]. Furthermore, the shift in the resonant frequency is not uniform for different fullerenes and their isomers. For example, He@C_{60} and He@C_{70} exhibit the ^{3}He shift at −6.40 and −28.82 ppm, while corresponding He@C_{60}^{6-} and He@C_{70}^{6-} ions resonate at −49.27 and 8.20 ppm [6–8]. Thus, the reduction may further help in the identification of the helium fullerenes, by e.g., re-measuring the spectra of the reduced systems.

We did not find any study on He@C_{84} anions except for Ref. [6] in which two signals at −22.12 and −22.80 ppm are assigned to unspecified He@C_{84} hexa-anions. Hence, we find it useful to report the calculated endohedral ^{3}He shift of the 23 isomers of hexa-anionic He@C_{84} in Table 1. All hexa-anions have closed-shell electronic structures. Indeed, the hexa-anionic species resonate most often far off the signal of the neutral species. Most of the anionic signals are within the range of −30 to −20 ppm which may complicate the

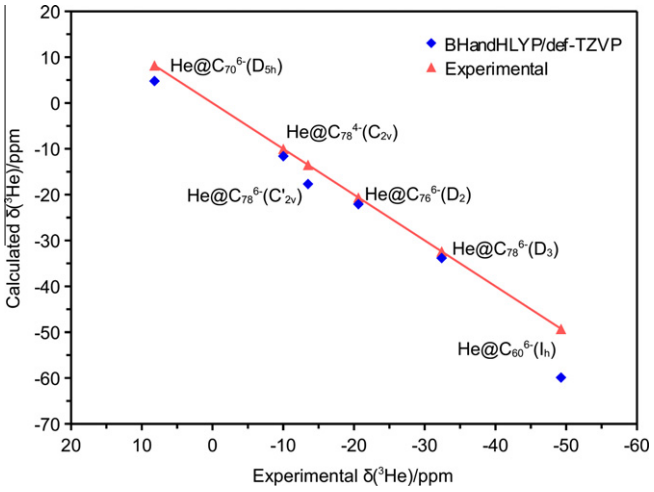

Figure 5. Calculated vs. experimental ^{3}He NMR shifts in a series of endohedral helium fullerene anions.

assignment. Looking at the ^{3}He shifts of the assigned neutral isomers and corresponding anions, a reduction of the experimental mixture should indeed lead to very different spectra, in which the corresponding anionic ^{3}He shifts may support the assignment of different isomers.

It is important to note, however, that the accuracy of the density functional methods (including the BHandHLYP/def-TZVP used in this study) is not so good for the anionic species as was for the neutral species, as seen in Figure 5. The computational results deviate typically by a few ppm but even a deviation of 10 ppm is observed for $He@C_{60}^{6-}$. This is probably due to the lack of a corresponding environment (solvent, counterion) in the gas phase calculations of anions. We postpone the issue of the counterion and solvent effects on the anionic species to future studies because of the complexity of the environment influence on NMR shifts [34]. The experimental resonances at −22.12 and −22.80 ppm are in the range in which the BHandHLYP/def-TZVP approach underestimates shielding by several ppm (Figure 5). Therefore, we can tentatively assign the anions to the isomers 22 and 23 with calculated ^{3}He shifts of −25.27 and −26.20 ppm, respectively.

4. Conclusions

We have shown that the ^{3}He NMR chemical shifts in the endohedral helium fullerenes can be predicted using the first principles density functional methods within the accuracy of 1 ppm without scaling or parameterization of the computational data. The accuracy of the computational levels used (BP86/def-TZVP for geometries and BHandHLYP/def-TZVP for ^{3}He shifts) is comparable to that exhibited by methods based on scaling of the computational data to experimental results. Such accuracy allows semi-quantitative assignment of the ^{3}He NMR spectra but can be problematic when the experimental shifts lie too close to each other. Further arguments, such as the relative isomer energy can be then used in assigning the spectra. Our approach allowed for assignment of the ^{3}He NMR spectra of the $He@C_{84}$ isomers in a mixture of endohedral helium fullerenes, primarily using the ^{3}He NMR shifts and the energy ordering. As additional criteria, we suggest calculations of the satellite minor signals caused by the corresponding di-helium system. Although computations can predict only the relative positions of the satellite peaks they may be helpful in the assignment. In addition, because the helium fullerenes reduced to the anionic states resonate at different frequencies than their neutral counterparts, the measurement of the NMR spectra of reduced isomers may lead to a more reliable assignment. Finally, we have predicted the ^{3}He NMR shifts for the so far unknown isomers of $He@C_{84}$ as well as for reduced $He@C_{84}^{6-}$ anions. For most isomers of $He@C_{84}$ their anions shield at substantially different frequencies than the neutral species.

Acknowledgement

This project was supported by the Academy of Sciences of the Czech Republic (Z04 055 905), Czech Science Foundation (grant no. 203/09/ 2037), and European Reintegration Grant (230955) within the 7th European Community Framework Program.

References

[1] P.W. Fowler, D.E. Manolopoulos, An Atlas of Fullerenes, Oxford University Press, Oxford, 1995.
[2] N. Tagmatarchis, A.G. Avent, K. Prassides, T.J.S. Dennis, H. Shinohara, Chem. Commun. (1999) 1023.
[3] T.J.S. Dennis, T. Kai, T. Tomiyama, H. Shinohara, Chem. Commun. (1998) 619.
[4] T.J.S. Dennis, T. Kai, K. Asato, T. Tomiyama, H. Shinohara, J. Phys.Chem. A 103 (1999) 8747.
[5] M. Saunders, R.J. Cross, H.A. Jiménez-Vázquez, R. Shimshi, A. Khong, Science 271 (1996) 1693.
[6] T. Sternfeld, M. Saunders, R.J. Cross, M. Rabinovitz, Angew. Chem. Int. Ed. 42 (2003) 3136.
[7] E. Shabtai et al., J. Am. Chem. Soc. 120 (1998) 6389.
[8] T. Sternfeld, R.E. Hoffman, M. Saunders, R.J. Cross, M.S. Syamala, M. Rabinovitz, J. Am. Chem. Soc. 124 (2002) 8786.
[9] J. Cioslowski, J. Am. Chem. Soc. 116 (1994) 3619.
[10] M. Bühl, C. van Wüllen, Chem. Phys. Lett. 247 (1995) 63.
[11] M. Bühl, W. Thiel, Chem. Phys. Lett. 233 (1995) 585.
[12] M. Bühl, M. Kaupp, O.L. Malkina, V.G. Malkin, J. Comput. Chem. 20 (1999) 91.
[13] Z. Chen, J. Cioslowsky, N. Rao, D. Moncrieff, M. Bühl, A. Hirsch, W. Thiel, Theor. Chem. Acc. 106 (2001) 364.
[14] Z. Chen, W. Thiel, Chem. Phys. Lett. 367 (2003) 15.
[15] J. Cioslowski, Chem. Phys. Lett. 227 (1994) 361.
[16] G.-W. Wang, X.-H. Zhang, H. Zhan, Q.-X. Guo, Y.-D. Wu, J. Org. Chem. (2003) 6732.
[17] G.-W. Wang, P. Wu, Theor. Chem. Acc. 123 (2009) 375.
[18] R.C. Haddon, A. Pasquarello, Phys. Rev. B 50 (1994) 16459. references therein.
[19] M. Straka, J. Vaara, J. Phys. Chem. A 110 (2006) 12338.
[20] G.-W. Wang, M. Saunders, A. Khong, R.J. Cross, J. Am. Chem. Soc. 122 (2000) 3216.
[21] M. Saunders et al., J. Am. Chem. Soc. 117 (1995) 9305.
[22] M. Straka, P. Lantto, J. Vaara, J. Phys. Chem. A 112 (2008) 2658.
[23] M. Hanni, P. Lantto, M. Iliaš, H.J.A. Jensen, J. Vaara, J. Chem. Phys. 127 (2007) 164313.
[24] R. Ahlrichs, M. Bär, M. Häser, H. Horn, C. Kölmel, Chem. Phys. Lett. 3 (1989) 165.
[25] A.D. Becke, Phys. Rev. A 38 (1988) 3098.
[26] J.P. Perdew, Phys. Rev. B 33 (1986) 8822.
[27] A. Schäfer, C. Huber, R. Ahlrichs, J. Chem. Phys. 1005829 (1994) 5829.
[28] K. Eichkorn, F. Weigend, O. Treutler, R. Ahlrichs, Theor. Chem. Acc. 97 (1997) 119.
[29] C. Lee, W. Yang, R.G. Parr, Phys. Rev. B 32 (1988) 785.
[30] A.D. Becke, J. Chem. Phys. 98 (1993) 1372.
[31] G. Sun, M. Kertesz, J. Phys. Chem. A 105 (2001) 5212.
[32] P. Štěpánek, M. Straka, unpublished results.
[33] Z. Chen, R.B. King, Chem. Rev. 105 (2005) 3613.
[34] M. Dračínský, P. Bouř, J. Chem. Theory Comput. 6 (2010) 288.